Chapter 6
Design and Evaluation of a New Solar Tower-Based Multi-generation System: Part II, Exergy and Exergoeconomic Modeling

Hamed Ghiasirad, Hadi Rostamzadeh, and Sajjad Nasri

Nomenclature

Symbols

C	Concentration ratio
h	Enthalpy (kJ. kg^{-1}), convection coefficient (W/m^{2}K)
K	Conductivity (W/m.K)
L	Length of tube (m)
S	Supercritical
T	Temperature (K), transcritical
V	Wind velocity (m/s)
X	Salinity (g. kg^{-1})

Abbreviations

F_r	View factor
HTR	High-temperature recuperator
HU	Heating unit
LTR	Low-temperature recuperator
MC	Main compressor
MFR	Mass flow ratio
PPTD	Pinch point temperature difference (K)

H. Ghiasirad (✉) · S. Nasri
Department of Mechanical Engineering, Faculty of Engineering, Sahand University
of Technology, Tabriz, Iran

H. Rostamzadeh
Energy and Environment Research Center, Niroo Research Institute (NRI), Tehran, Iran

RC   Recompression compressor
STP   Solar tower power

Greek Letters
δ   Thickness (m)
ε   Effectiveness, emissivity
η Efficiency (%)
λ Conductivity (W/m.K)
μ Viscosity (Pa.s)
ω Humidity
ρ Reflectivity, density (kg/m^3)

Subscripts and Superscripts
Ape   Aperture
em   Emissive
Dhum   Dehumidifier
fc   Forced convection
Gen   Generator
Hum   Humidifier
H, Hel   Heliostat
Insi   Inner side of receiver
Insu   Insulation
is   Isentropic
ms   Molten salt
nc   Natural convection
ref   Reflection
Sur   Surface
sw   Sea water
TC   Transcritical compressor
W   Wall

6.1 Introduction

Exergy has been introduced as a conceptual tool in the design of more efficacious energy systems when the performance of the system should be judged by evaluating it relative to a reference state. Broadly speaking, exergy is defined as a maximum available work that a unit can do while interacting with the ambient [1]. Therefore, thermodynamic properties of the ambient can be inferred as the reference state through the exergy analysis. An intensive and accurate exergy analysis based on practical assumptions will lead to recognition of the main source of the losses occurring through the operation of the system both qualitatively and quantitatively. This is the main distinctive feature of exergy analysis, which is wanted in energy

analysis. The quantitative feature of exergy analysis refers to avoidance of thermodynamic imperfection in different elements of a system by spotlighting the causes and locations of these imperfections for redesign purposes [2].

Exergoeconomic is the combination of exergy analysis and cost estimation based on exergy values at each state. Application of exergoeconomic in energy systems mainly aims at designing more sustainable units in terms of waste handling by considering cost and the source of irreversibility. Basically, the main aim of exergoeconomic analysis can be categorized as follows [3] :

- The source, location, and magnitude of the cost destructed or lost in an energy system can be determined.
- To assess the overall cost of a multi-generation system or individual cost associated with each product.
- To make a multi-objective optimization of a complex system more feasible since an overall unit cost can be defined for the entire system.
- To expand the decision-making procedures into more viable analysis such as reliability and risk evaluation based upon the obtained cost index.
- To justify the initial design process of the devised setup evaluated based on the energy and exergy concepts by comparing it to similar systems where their cost index is more encouraging.

Application of exergoeconomic analysis in multi-generation systems (the conceptual definition of a multi-generation system is presented in Chap. 5) can be satisfactory based upon the above-categorized reasons. In multi-generation systems, each state experiences a series of complex thermodynamic processes, where determination of thermodynamic properties at each state can provide favorable information for designers. The same merit can be found in exergy and exergoeconomic analysis since exergy rate and cost rate associated with each state can be determined. This detail evaluation in terms of cost can be much more than an asset since present modern marketing in energy management profusely emphasizes on more viable ideas that are based on more accurate and detail cost data. Future plans on ameliorating performance and cost of the current combined power plants will more intensively be centralized on developing multi-generation systems that are more efficient and economical in their different utility sectors. As pinpointed in Chap. 5, a multi-generation system can be constructed in two forms: combined or integrated. Depending on which classification the designed multi-generation system is set on, the cost rate manipulation in terms of decreasing overall cost of the unit can be more or less complex. This is partly because of minor constructive development in exergoeconomic analysis of multi-generation systems. The objective is even highly imperative when the design layout includes a competitive heat source, especially a reliable renewable source such as solar energy. Even though the intermittency of solar irradiance through the nights or low-temperature periods of a year is questionable (which makes the cost-benefit of the proposal at stake), recent advances in development of high-tech storage energy devices and materials have proved the cost profitability of the solar-based multi-generation systems from mathematical-based cost models like exergoeconomic. Therefore, it is crucial to further discuss economic

perspectives of the devised new solar-based multi-generation system elaborated in previous chapter from energy viewpoint. Before we proceed further in the construction of a robust exergoeconomic model for the designed multi-generation system, it is important to look around the most recent constructed integrated/combined energy systems from exergoeconomic viewpoint. The only study in exergoeconomic of multi-generation systems in solar-based multi-generation system is the study of Leiva-Illanes et al. [4]. According to Ref. [4], authors carried out exergoeconomic analysis of a new solar-based multi-generation system and suggested the best configuration in terms of unit exergy cost. They found that the high portion of cost associated to the system (in order) is the solar collectors, evaporator, and reheater. They also deduced that the devised solar-based multi-generation system is more economical than the stand-alone setup. With their devised layout, the unit exergy cost associated with electricity, cooling, water, and heating were declined by 6.8%, 45.6%, 59.2%, and 32.2%, respectively.

In the light of reviewed literature and based on the results of previous chapter, it can be figured out that no study has been carried out to study exergoeconomic analysis of a high-efficient multi-generation system operated by a solar tower power (STP) plant up to yet. The only study was Leiva-Illanes et al. [4] in which they used solar collectors applicable for low-temperature combined plants. To cover this shortcoming of the existing literature works, exergoeconomic analysis of the devised solar-based multi-generation system in the first part of this study is investigated in this chapter. The rest of this chapter is arranged in the following order. In Sect. 6.2, all employed mathematical relations and presumptions related to exergy and exergoeconomic analysis are displayed. In the third sub-section, results are presented and discussed extensively. Finally, some concluding comments from economic vantage point are listed in the last part.

6.2 Materials and Methods

In this part, exergy and exergoeconomic presumptions and relations are intensively presented. In the first subsection, exergy concept and the relations associated with it are presented. In the second subsection, exergoeconomic analysis is elaborated in detail. Ultimately, the main cost parameters are extended.

6.2.1 Exergy Analysis

In this study, only physical and chemical exergies are considered through exergy assessment [1]. The exergy-based balance relation for individual constituent of a system may be articulated in the sense of the all exiting and entering exergy rates of the constituents as follows:

$$\dot{Ex}_{D,k} = \dot{Ex}_{F,k} - \dot{Ex}_{P,k} - \dot{Ex}_{L,k} \tag{6.1}$$

Disregarding the inconsequential impact of the potential and kinetic exergies of all flows, the total exergy of the kth fluid stream is articulated as follows [5] :

$$\dot{Ex}_k = \dot{Ex}_{ph,k} + \dot{Ex}_{ch,k} \tag{6.2}$$

where:

$$\dot{Ex}_{ph,k} = \dot{m}(h - h_0 - T_0(s - s_0))_k \tag{6.3}$$

$$\dot{Ex}_{ch,MS} = \dot{m}\left(0.6\left[\frac{ex^0_{ch,NaNO_3}}{M_{NaNO_3}}\right] + 0.4\left[\frac{ex^0_{ch,KNO_3}}{M_{KNO_3}}\right]\right) \tag{6.4}$$

$$\dot{Ex}_{ch,Water,CO_2} = \dot{m}\left(\left[\frac{ex^0_{ch,Water,CO_2}}{M_{Water,CO_2}}\right]\right) \tag{6.5}$$

in which, 0 refers to the environment condition. To compute saline water exergy, pressure-based correlations accessible in EES software are used [6, 7]. Exergy of humid air is computed from Eq. (6.6) [8]:

$$\begin{aligned} ex_{da} &= (c_{p,a} + \omega c_{p,v})T_0\left(\frac{T}{T_0} - 1 - \ln\frac{T}{T_0}\right) + (1 + 1.608\omega)R_aT_0\ln\frac{P}{P_0} \\ &+ R_aT_0(1 + 1.608\omega)\ln\frac{1 + 1.608\omega_0}{1 + 1.608\omega} + 1.608\omega\ln\frac{\omega}{\omega_0} \end{aligned} \tag{6.6}$$

where, $R_a = 0.287$ (kJ/kg. K) and ω is the humidity ratio:

$$\omega = \frac{\dot{m}_v}{\dot{m}_a} \tag{6.7}$$

The exergetic efficiency for each constituent of a system may be articulated as follows:

$$\eta_{ex,k} = \frac{\text{Exergy of product}}{\text{Total supplied exegy}} = \frac{\dot{Ex}_{out}}{\dot{Ex}_{in}} = \frac{\dot{Ex}_{P,k}}{\dot{Ex}_{F,k}} \tag{6.8}$$

Based upon the above-defined relations, the exergy balance equations for different constituents of the suggested multi-generation system are presented in Table 6.1.

Table 6.1 The exergy balance equations for different constituents of the suggested multi-genera-tion system

Constituents	Fuel	Product	Loss
Hel	$\dot{Q}_{Hel}\left(1 - \frac{T_0}{T_{sun}}\right)$	$\dot{Q}_{Rec}\left(1 - \frac{T_0}{T_{sun}}\right)$	–
Rec	$\dot{Q}_{Rec}\left(1 - \frac{T_0}{T_{sun}}\right)$	$\dot{Ex}_1 - \dot{Ex}_2$	$\dot{Q}_{Rec,Loss}\left(1 - \frac{T_0}{T_{Rec}}\right)$
Gen	$\dot{Ex}_1 - \dot{Ex}_2$	$\dot{Ex}_3 - \dot{Ex}_{19}$	–
Tur	$\dot{Ex}_3$	$\dot{Ex}_4 + \dot{W}_{Tur}$	–
HTR	$\dot{Ex}_4 - \dot{Ex}_5$	$\dot{Ex}_{19} - \dot{Ex}_{18}$	–
LTR	$\dot{Ex}_5 - \dot{Ex}_6$	$\dot{Ex}_{17} - \dot{Ex}_{16}$	–
HU	$\dot{Ex}_9 - \dot{Ex}_{10}$	$\dot{Ex}_{12} - \dot{Ex}_{11}$	–
DHW	$\dot{Ex}_{10} - \dot{Ex}_{13}$	$\dot{Ex}_{15} - \dot{Ex}_{14}$	–
MC	$\dot{Ex}_{13} + \dot{W}_{MC}$	$\dot{Ex}_{16}$	–
RC	$\dot{Ex}_7 + \dot{W}_{RC}$	$\dot{Ex}_8$	–
TC	$\dot{Ex}_{27} + \dot{W}_{TC}$	$\dot{Ex}_{20}$	–
GC	$\dot{Ex}_{20} - \dot{Ex}_{21}$	$\dot{Ex}_{30} - \dot{Ex}_{29}$	–
IHX	$\dot{Ex}_{21} - \dot{Ex}_{22}$	$\dot{Ex}_{27} - \dot{Ex}_{24}$	–
TV	$\dot{Ex}_{22}$	$\dot{Ex}_{23}$	–
Eva	$\dot{Ex}_{23} - \dot{Ex}_{24}$	$\dot{Ex}_{26} - \dot{Ex}_{25}$	–
Hum	$\dot{Ex}_{30}$	$\dot{Ex}_{33} - \dot{Ex}_{32}$	$\dot{Ex}_{31}$
Dhum	$\dot{Ex}_{33} - \dot{Ex}_{32}$	$\dot{Ex}_{29} - \dot{Ex}_{28} + \dot{Ex}_{34}$	–

6.2.2 Exergoeconomic Analysis

The balance equation based on the cost of the kth constituent of a system is articulated as follows [1]:

$$\dot{C}_{q,k} + \sum \dot{C}_{in,k} + \dot{Z}_k = \dot{C}_{w,k} + \sum \dot{C}_{out,k} \qquad (6.9)$$

where, the utilized parameters are:

$\dot{C}_{in,k}$: stands for the cost rate of the incoming stream of the kth constituent.
$\dot{C}_{out,k}$: stands for the cost rate of the outcoming stream of the kth constituent.
$\dot{C}_{w,k}$: stands for the cost rate of work.
$\dot{C}_{q,k}$: stands for the cost rate of heat transfer.

Exergy and cost rate are related as follows [1]:

$$\dot{C}_k = c_k \dot{Ex}_k \qquad (6.10)$$

The overall cost rate of the kth constituent of a system is articulated as follows [1]:

$$\dot{Z}_k = \dot{Z}_k^{CI} + \dot{Z}_k^{OM} = \frac{PEC_k \times \phi_c \times CRF}{\tau} \tag{6.11}$$

where:

$\dot{Z}_k^{CI}$: stands for the capital investment cost of the kth constituent.
$\dot{Z}_k^{OM}$: stands for the operating and maintenance cost of the kth constituent.
τ: stands for the annual operating hours.
ϕ_c: stands for the maintenance factor.
PEC_k: stands for the purchase cost of the kth constituent.
CRF: stands for the capital recovery factor.

CRF is attained from Eq. (6.12) [1]:

$$CRF = \frac{i(1+i)^{n_r}}{(1+i)^{n_r} - 1} \tag{6.12}$$

where:

i: stands for the interest rate.
n_r: stands for the total operating years of the system.

The cost rate of exergy destruction of the kth constituent is articulate as follows [1]:

$$\dot{C}_{D,k} = c_{F,k}\dot{Ex}_{D,k}\left(\text{If } \dot{Ex}_{P,k} = \text{constant}\right) \tag{6.13}$$

The relative cost difference (r_k) and exergoeconomic factor (f_k) for the kth component of a system may be expressed, respectively, as [1] follows:

$$r_k = (c_{P,k} - c_{F,k})/c_{F,k} \tag{6.14}$$

$$f_k = \dot{Z}_k/(\dot{Z}_k + \dot{C}_{D,k}) \tag{6.15}$$

The detail cost balance relations and purchase equipment cost (PEC) for each constituent of the devised multi-generation system are presented in Tables 6.2 and 6.3.

Some central exergy and economic parameters required for analysis are presented in Table 6.4.

Assuming the logarithmic mean temperature difference (LMTD) and the total heat transfer coefficient, the total heat exchanger area might be attained from the equation below:

$$A_k = \frac{\dot{Q}_k}{U_k \Delta T_{LMTD}} \tag{6.16}$$

Table 6.2 Purchase equipment cost (PEC) for each constituent of the devised multi-generation system

Constituents	PEC_{2018} [9]	Ref.
Hel	$PEC_{2009\to2018} = \left(\frac{638.1}{521.9}\right) \times 216\,A_h$	[10]
Rec	$PEC_{2009\to2018} = \left(\frac{638.1}{521.9}\right) \times 3.52 \times 10^6 \times \left(\frac{\dot{Q}_{Rec,Abs}}{1000}\right)^{0.44}$	[10]
Tower	$PEC_{2009\to2018} = \left(\frac{638.1}{521.9}\right) \times 30.5\dot{Q}_{Rec,Abs} + 961000$	[10]
Gen HTR LTR HU DHW GC IHX Eva	$P_{Gen}[\text{bar}] = P_{19} - 1,\ P_{HTR} = P_{18} - 1,\ P_{LTR} = P_{17} - 1,\ P_{HU} = P_9 - 1$ $P_{DHW} = P_{10} - 1,\ P_{GC} = P_{20} - 1,\ P_{IHX} = P_{21} - 1,\ P_{Eva} = P_{24} - 1$ $PEC_{1996\to2018} = \left(\frac{638.1}{381.7}\right) \times Z_0(1.63 + 1.66F_P)$ $\log_{10}(Z_0) = 4.3247 - 0.303\log_{10}(A) + 0.1634(\log_{10}(A))^2$ $\log_{10}(F_P) = 0.03881 - 0.11127\log_{10}(P_K) + 0.0818(\log_{10}(P_K))^2$	[11]
Tur	$PEC_{1996\to2018} = \left(\frac{638.1}{381.7}\right) \times Z_0 3.5\, Z_{0,Tur}$ $\log_{10}(Z_{0,Tur}) = 2.7051 - 1.4398\log_{10}(\dot{W}_{Tur}) - 0.1776\left(\log_{10}(\dot{W}_{Tur})\right)^2$	[11]
MC RC TC	$PEC_{1996\to2018} = \left(\frac{638.1}{381.7}\right) \times 3.8\, Z_{0,Com}$ $\log_{10}(Z_{0,Com}) = 2.2897 - 1.3604\log_{10}(\dot{W}_{Com}) - 0.1027\left(\log_{10}(\dot{W}_{Com})\right)^2$	[11]
TV	$PEC_{2000\to2018} = \left(\frac{638.1}{394.1}\right) \times 114.5\, \dot{m}_{22}$	[12]
Hum	$PEC_{2012\to2018} = \left(\frac{638.1}{584.6}\right) \times 133\left(\frac{\dot{m}_{FW}}{0.0015}\right)^{0.6}$	[13]
Dhum	$PEC_{2012\to2018} = \left(\frac{638.1}{584.6}\right) \times 70\left(\frac{\dot{m}_{FW}}{0.0015}\right)^{0.6}$	[13]

Table 6.3 Cost balances and auxiliary equations for each constituent of the devised multi-generation system

Constituents	Cost balance	Auxiliary equation
Hel	$\dot{C}_{in,Hel} + \dot{Z}_{Hel} = \dot{C}_{in,Rec}$	$c_{in,\,Hel} = 0$
Rec	$\dot{C}_2 + \dot{C}_{in,Rec} + \dot{Z}_{Tower} + \dot{Z}_{Rec} = \dot{C}_1$	–
Gen	$\dot{C}_1 + \dot{C}_{19} + \dot{Z}_{Gen} = \dot{C}_2 + \dot{C}_3$	$c_2 = c_1$
Tur	$\dot{C}_3 + \dot{Z}_{Tur} = \dot{C}_4 + \dot{C}_{W,Tur}$	$c_4 = c_3$
HTR	$\dot{C}_{18} + \dot{C}_4 + \dot{Z}_{HTR} = \dot{C}_{19} + \dot{C}_5$	$c_5 = c_4$
LTR	$\dot{C}_{16} + \dot{C}_5 + \dot{Z}_{LTR} = \dot{C}_{17} + \dot{C}_6$	$c_6 = c_5$
Division point	$\dot{C}_6 = \dot{C}_9 + \dot{C}_7$	$c_9 = c_7$
HU	$\dot{C}_{11} + \dot{C}_9 + \dot{Z}_{HU} = \dot{C}_{10} + \dot{C}_{12}$	$c_{10} = c_9$ $c_{11} = 0$
DHW	$\dot{C}_{10} + \dot{C}_{14} + \dot{Z}_{DHW} = \dot{C}_{15} + \dot{C}_{13}$	$c_{13} = c_{10}$ $c_{14} = 0$
MC	$\dot{C}_{W,MC} + \dot{C}_{13} + \dot{Z}_{MC} = \dot{C}_{16}$	$c_{W,\,MC} = c_{W,\,Tur}$
RC	$\dot{C}_{W,RC} + \dot{C}_7 + \dot{Z}_{RC} = \dot{C}_8$	$c_{W,\,RC} = c_{W,\,Tur}$
TC	$\dot{C}_{W,TC} + \dot{C}_{27} + \dot{Z}_{TC} = \dot{C}_{20}$	$c_{W,\,TC} = c_{W,\,Tur}$
GC	$\dot{C}_{20} + \dot{C}_{29} + \dot{Z}_{GC} = \dot{C}_{21} + \dot{C}_{30}$	$c_{21} = c_{20}$
IHX	$\dot{C}_{21} + \dot{C}_{24} + \dot{Z}_{IHX} = \dot{C}_{22} + \dot{C}_{27}$	$c_{22} = c_{21}$
TV	$\dot{C}_{22} + \dot{Z}_{TV} = \dot{C}_{23}$	–
Eva	$\dot{C}_{23} + \dot{C}_{25} + \dot{Z}_{Eva} = \dot{C}_{24} + \dot{C}_{26}$	$c_{23} = c_{24}$ $c_{25} = 0$
Hum	$\dot{C}_{30} + \dot{C}_{32} + \dot{Z}_{Hum} = \dot{C}_{31} + \dot{C}_{33}$	$c_{30} = c_{31}$ $c_{32} = c_{33}$
Dhum	$\dot{C}_{28} + \dot{C}_{33} + \dot{Z}_{Dhum} = \dot{C}_{34} + \dot{C}_{32} + \dot{C}_{29}$ $\frac{\dot{C}_{32} - \dot{C}_{28}}{\dot{Ex}_{32} - \dot{Ex}_{28}} = \frac{\dot{C}_{29} - \dot{C}_{28}}{\dot{Ex}_{29} - \dot{Ex}_{28}}$	$c_{28} = 0$

Table 6.4 Some required exergy and economic parameters for exergoeconomic evaluation of the proposed multi-generation system [14]

Parameters	Value	Ref.
Annual number of hours, τ (hr)	4800	[5]
Components' expected life, n_r (years)	30	[5]
Maintenance factor, $\varnothing_c$	1.02	[5]
Interest rate, i	0.08	[5]
ex^0_{ch,KNO_3}, (kJ/kmol)	−15,290	[15]
$ex^0_{ch,NaNO_3}$, (kJ/kmol)	−15,745	[15]
ex^0_{ch,CO_2}, (kJ/kmol)	14,176	[15]
$ex^0_{ch,water}$, (kJ/kmol)	45	[15]

Table 6.5 The overall heat transfer coefficient for heat exchangers

Component	U (kW/m^{2}K)	Ref.
Gen and HTR	3	[16]
LTR	1.6	[16]
HU	1.6	[16]
DHW	2	[16]
GC	0.3	[11]
Eva	1.5	[11]
IHX	1	[11]

The total heat transfer coefficients for each heat exchanger are tabulated in Table 6.5. The updated cost rates for each individual component would be updated as follows:

$$\text{Original cost} = \text{Cost at reference year} \times \frac{\text{Cost index for the original year}}{\text{Cost index for the reference year}} \quad (6.17)$$

6.2.3 Main Exergy and Cost Parameters

The second-law efficiency of the proposed poly-generation system can be written as follows:

$$\eta_{\text{ex}} = \frac{\dot{W}_{\text{net}} + \dot{\text{Ex}}_{\text{P,HU}} + \dot{\text{Ex}}_{\text{P,DHW}} + \dot{\text{Ex}}_{\text{P,Eva}} + \dot{\text{Ex}}_{\text{Desal}}}{\dot{\text{Ex}}_{\text{F,Hel}}} \quad (6.18)$$

where, fuel and product exergy rates are listed in Table 6.1 and desalination exergy rate is given by Eq. (6.19):

$$\dot{\text{Ex}}_{\text{Desal}} = \dot{\text{Ex}}_{\text{FW}} - \dot{\text{Ex}}_{\text{SW}} \quad (6.19)$$

System total cost rate ($\dot{C}_{\text{sys}}$) for the devised multi-generation system can be expressed as follows:

$$\dot{C}_{\text{sys}} = \dot{C}_1 + \dot{Z}_{\text{tot}} \quad (6.20)$$

where, $\dot{Z}_{\text{tot}}$ is the total investment and operating cost rate and $\dot{C}_1$ is the high-temperature molten salt cost.
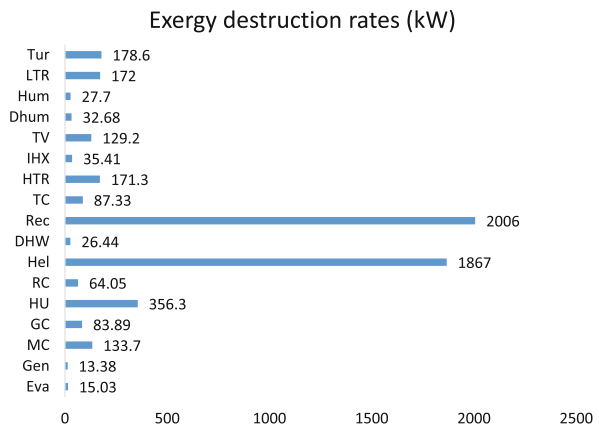
6.3 Results and Discussion

Table 6.6 presents results of exergy and exergoeconomic analysis of the devised multi-generation system described in Chap. 5. According to Table 6.6, exergy efficiency of the proposed MGS is computed 21.45%. Also, among all subsystems, heliostat field has the exergy of fuel of 7470 kW. The total investment cost of the whole system is estimated 433.2 $/h. Moreover, the overall cost rate of the setup was calculated 743.2 $/h. Figure 6.1 indicates results of exergy destruction for all elements available in the system. Accordingly, the receiver has a pivotal role in the overall exergy destruction by exergy destruction of 2006 kW, followed by heliostat by 1867 kW.

Table 6.6 The significant results of exergy and economic analysis

Parameter	Value
$\dot{Ex}_{F,Hel}$ (kW)	7470
$\dot{Ex}_{P,HU}$ (kW)	236.1
$\dot{Ex}_{P,DHW}$ (kW)	25.13
$\dot{Ex}_{Desal}$ (kW)	2.8
η_{ex} (%)	21.45
$\dot{Z}_{tot}$ (/h)	433.2
$c_{W, Tur}$ ($/GJ)	43.06
$\dot{C}_{sys}$ (/h)	743.2

Fig. 6.1 Exergy destruction rates of each component of multi-generation system

Exergy destruction rates (kW)

Component	Value
Tur	178.6
LTR	172
Hum	27.7
Dhum	32.68
TV	129.2
IHX	35.41
HTR	171.3
TC	87.33
Rec	2006
DHW	26.44
Hel	1867
RC	64.05
HU	356.3
GC	83.89
MC	133.7
Gen	13.38
Eva	15.03

6.4 Parametric Study

6.4.1 Effect of Direct Normal Irradiance

In this sub-section, some parameters are studied to obtain their effect on exergy efficiency and total cost rate of the system. In the beginning, effect of direct normal irradiance (DNI) can be seen in Fig. 6.2, in which, with increasing DNI, exergy efficiency and total cost rate increase. With increasing DNI, cooling and desalination product exergies are constant, but product exergy of heating, DHW, and net electricity have higher increase than solar exergy input, and for this reason, the second-law efficiency will be increased. On the other hand, the total investment cost rate and cost rate of stream 1 have linear increase. So, there is a linear increase in the total cost rate. Hence, DNI should be optimized for simultaneous high exergy efficiency and low total cost rate.

6.4.2 Effect of Receiver Concentration Ratio

Receiver concentration ratio is a critical parameter because of its impacts on receiver surface temperature, conduction, convection, and radiation energy losses. Its impact is shown in Fig. 6.3, wherein its enhancement creates higher energy efficiency. With growing receiver concentration ratio, receiver surface temperature and aperture area get larger and fall off, respectively. Enhancement of the receiver temperature causes a few increases of heat losses. On the other hand, decrease of aperture area causes high decrease of heat losses. So, decrease of heat losses is a suitable reason in
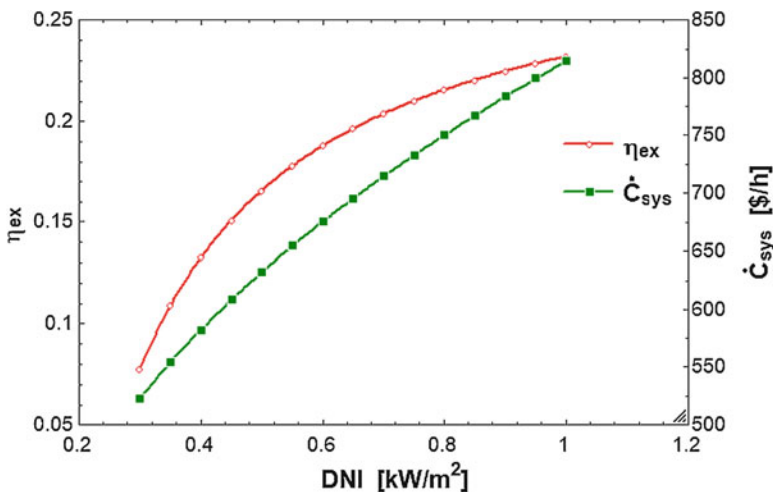

Fig. 6.2 Effect of DNI on exergy efficiency and total cost rate of the system
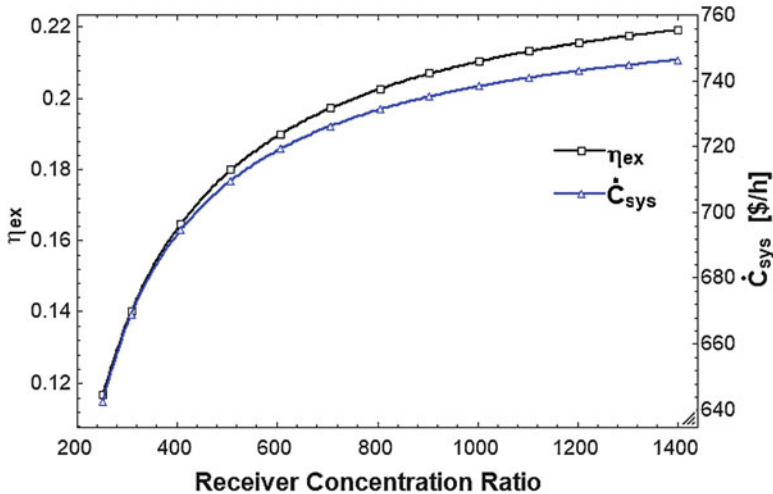
Fig. 6.3 Effect of receiver concentration ratio on exergy efficiency and total cost rate of the system

increasing exergy efficiency. Also, investment cost and fuel cost rates of stream 1 have an enhancement with increment of concentration ratio. Decrease of this effect is heat loss reduction and absorbed heat transfer of receiver, investment cost of receiver and tower, and mass flow of stream 1 enhancement. So, it is a good idea to optimize concentration ratio for two objective functions.

6.4.3 Effect of Generator Pinch Point Temperature Difference

According to Fig. 6.4, with increasing generator PPTD, exergy efficiency and total cost rate will be decreased and increased, respectively. Because cooling, desalination and solar exergy values are constant and heating, DHW and net electricity product exergy rates have a slight decrease. So, there is a few decreases in the second-law efficiency. With increasing generator PPTD, the total capital cost is almost constant, but $\dot{C}_1$ has a high increase, and for this reason, the total cost rate will be increased.

6.4.4 Effect of MC and RC Pressure Ratio

Pressure ratio of compressors is an important parameter because its increment has a considerable effect on power consumption and investment cost. Figure 6.5 shows its effect on main objectives. According to the figure, pressure ratio around 4 is the best
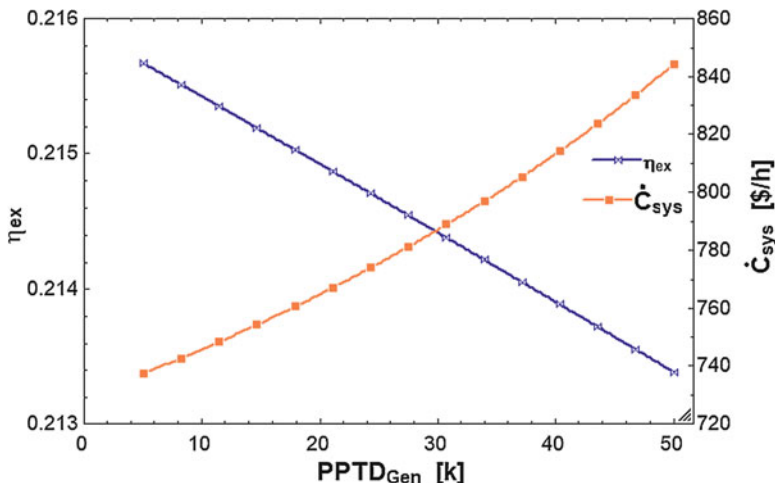
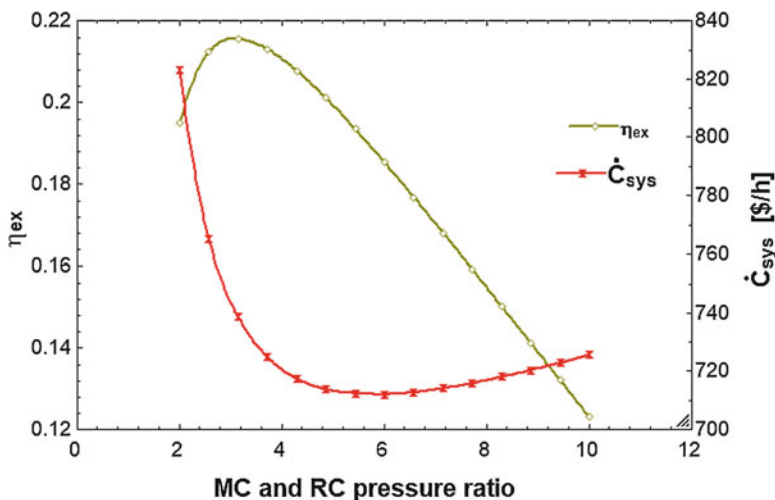**Fig. 6.4** Effect of generator PPTD on exergy efficiency and total cost rate of the system

Fig. 6.5 Effect of MC and RC pressure ratio on exergy efficiency and total cost rate of the system

option to maximize exergy efficiency and minimize total cost rate. With increasing pressure ratio, cooling, desalination, and solar exergy rates are constant, and net electricity and DHW exergy rates have decreased, but heating exergy rate will be increased. Also, there is a high decrease in $\dot{C}_1$ and small increase in the total capital costs. These decrease and increase of various values cause to have an optimal point in Fig. 6.5.

6.4.5 Effect of HTR, LTR, Hum, and Dhum Effectiveness

Effectiveness is one of significant parameters that has more effect on main products because it has the same value for HTR, LTR, Hum, and Dhum. It is obvious that high effectiveness values cause high proficiency of heat exchangers, superior exergy efficiency, and further total cost rate. So, effectiveness should be optimized in order to obtain good objective functions simultaneously (Fig. 6.6).

6.4.6 Effect of Ambient, Water, and Seawater Inlet Temperatures

According to Fig. 6.7, ambient temperature is one of most important parameters that plays a significant role in main objectives. Also, ambient temperature has the same value as DHW and HU inlet water temperatures and seawater inlet temperature to the HDH system. Because of the existing environment temperature in negative part of exergy formulas, all streams' exergy rates will be decreased with the enhancement of ambient temperature, and for this reason, exergy efficiency decreases. On the other hand, $\dot{C}_1$ has small reduction, but $\dot{Z}_{tot}$ has high enhancement, and these behaviors cause to increase the total cost rate. So, in this result, it can be obtained that the proposed system should be created in cold regions.
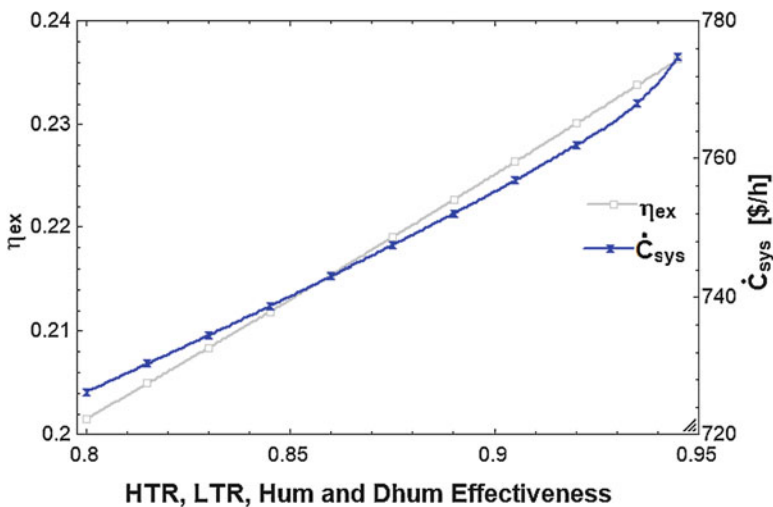

Fig. 6.6 Effect of HTR, LTR, Hum, and Dhum effectiveness on exergy efficiency and total cost rate of the system
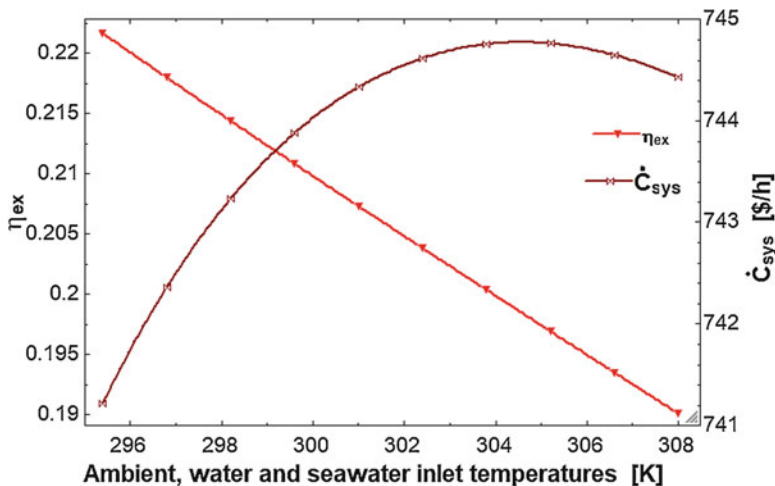
Fig. 6.7 Effect of ambient, water, and seawater inlet temperatures on exergy efficiency and total cost rate of the system

6.4.7 Effect of T-CO2 Compressor to Turbine Electricity Ratio

Electricity consumption of T-CO2 compressor is one of the principal parameters that impacts on exergy efficiency and total cost rate. By enhancement of work ratio, solar, heating and DHW exergy rates are not changed, but net power output has large reduction than cooling and desalination exergy rate enhancement. So, according Fig. 6.8, increment of electricity ratio causes reduction of the second-law efficiency. On the other hand, $\dot{C}_1$ is invariant, and total investment costs have enhancement due to increasing of power consumption of T-CO2 compressor and mass flow rates of cooling and desalination units. So, in small electricity ratios, the proposed system has suitable performance.

6.5 Concluding Comments

Exergy and exergoeconomic analysis of a multi-generation system operating with a solar tower power (STP) plant was carried out in this chapter. It was found that using STP plant as a prime mover of a multi-generation system leads to encouraging results, notwithstanding less attention is paid in this regard in comparison with direct capturing of solar irradiance via solar collectors. The following major results are extracted through the study:
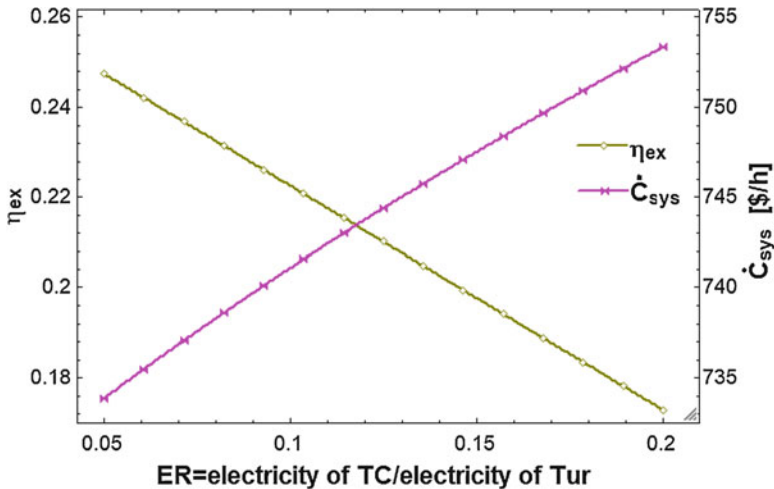
Fig. 6.8 Effect of T-CO2 compressor to turbine electricity ratio on exergy efficiency and total cost rate of the system

- The receiver had a pivotal role in the overall exergy destruction by exergy destruction of 2006 kW, followed by heliostat with exergy destruction of 1867 kW.
- The overall exergy efficiency and cost of the system were computed 21.45% and 743.2 $/h, respectively.
- It was discerned that exergy efficiency can be raised up from the base value with the rise of direct normal irradiance (DNI), receiver concentration ratio, and heat exchangers effectiveness or with the decrease of the generator pinch point temperature, ambient temperature, and amount of electricity supplied to the transcritical CO_2 refrigeration cycle.
- The overall cost rate parameter can be decreased by decreasing the amount of electricity supplied to the transcritical CO_2 refrigeration cycle, heat exchangers effectiveness, generator pinch point temperature, DNI, and receiver concentration ratio.

References

1. Bejan, A., & Tsatsaronis, G. (1996). *Thermal design and optimization*. John Wiley & Sons, USA.
2. Bejan, A. (2016). *Advanced engineering thermodynamics*. John Wiley & Sons, USA.
3. Tsatsaronis, G. (1993). Thermoeconomic analysis and optimization of energy systems. *Progress in Energy and Combustion Science, 19*(3), 227–257.

4. Leiva-Illanes, R., et al. (2019). Exergy cost assessment of CSP driven multi-generation schemes: Integrating seawater desalination, refrigeration, and process heat plants. *Energy Conversion and Management, 179*, 249–269.

5. Ma, Y., et al. (2019). Optimal integration of recompression supercritical CO2 Brayton cycle with main compression intercooling in solar power tower system based on exergoeconomic approach. *Applied Energy, 242*, 1134–1154.

6. Nayar, K. G., Sharqawy, M. H., & Banchik, L. D. (2016). Thermophysical properties of seawater: A review and new correlations that include pressure dependence. *Desalination, 390*, 1–24.

7. Sharqawy, M. H., Lienhard, J. H., & Zubair, S. M. (2010). Thermophysical properties of seawater: A review of existing correlations and data. *Desalination and Water Treatment, 16* (1–3), 354–380.

8. Wepfer, W., Gaggioli, R., & Obert, E. (1979). Proper evaluation of available energy for HVAC. *ASHRAE Transactions, 85*(1), 214–230.

9. CEPCI. (2016). Chemical engineering plant cost index. *Chemical Engineer*. www.chemengonline.com.

10. Nathan, G., Battye, D., & Ashman, P. (2014). Economic evaluation of a novel fuel-saver hybrid combining a solar receiver with a combustor for a solar power tower. *Applied Energy, 113*, 1235–1243.

11. Ipakchi, O., Mosaffa, A., & Farshi, L. G. (2019). Ejector based CO2 transcritical combined cooling and power system utilizing waste heat recovery: A thermoeconomic assessment. *Energy Conversion and Management, 186*, 462–472.

12. Rostamzadeh, H., et al. (2018). Exergoeconomic optimisation of basic and regenerative triple-evaporator combined power and refrigeration cycles. *International Journal of Exergy, 26*(1–2), 186–225.

13. Sayyaadi, H., & Ghorbani, G. (2018). Conceptual design and optimization of a small-scale dual power-desalination system based on the Stirling prime-mover. *Applied Energy, 223*, 457–471.

14. Gholizadeh, T., Vajdi, M., & Mohammadkhani, F. (2019). Thermodynamic and thermoeconomic analysis of basic and modified power generation systems fueled by biogas. *Energy Conversion and Management, 181*, 463–475.

15. Kotas, T. J. (2013). *The exergy method of thermal plant analysis*. John Wiley & Sons, USA.

16. Wang, X., & Dai, Y. (2016). Exergoeconomic analysis of utilizing the transcritical CO2 cycle and the ORC for a recompression supercritical CO2 cycle waste heat recovery: A comparative study. *Applied Energy, 170*, 193–207.